Global Change Biology (2004) **10,** 683–692, doi: 10.1111/j.1529-8817.2003.00754.x

Teleconnection between tree growth in the Amazonian floodplains and the El Niño–Southern Oscillation effect

JOCHEN SCHÖNGART*, WOLFGANG J. JUNK†, MARIA TERESA F. PIEDADE‡, JOSÉ MARCIO AYRES§[1], ALOYS HÜTTERMANN¶, and MARTIN WORBES*

Institute of Agronomy in the Tropics, University of Göttingen, Grisebachstrasse 6, 37077 Göttingen, Germany, †Max-Planck-Institute for Limnology, Postfach 165, 24302 Plön, Germany, ‡Instituto Nacional de Pesquisas da Amazônia (INPA), CP 478, 69.011-970 Manaus, AM, Brazil, §Instituto de Desenvolvimento Sustentável Mamirauá, CP 38, 69.470-000 Tefé, AM, Brazil, ¶Institute of Forest Botany, University of Göttingen, Büsgenweg 2, 37077 Göttingen, Germany

Abstract

There is a limited knowledge about the El Niño–Southern Oscillation (ENSO) effects on the Amazon basin, the world's largest tropical rain forest and a major factor in the global carbon cycle. Seasonal precipitation in the Andean watershed annually causes a several month-long inundation of the floodplains along the Amazon River that induces the formation of annual rings in trees of the flooded forests. Radial growth of trees is mainly restricted to the nonflooded period and thus the ring width corresponds to its duration. This allows the construction of a tree-ring chronology of the long-living hardwood species *Piranhea trifoliata* Baill. (Euphorbiaceae). El Niño causes anomalously low precipitation in the catchment that results in a significantly lower water discharge of the Amazon River and consequently in an extension of the vegetation period. In those years tree rings are significantly wider. Thus the tree-ring record can be considered as a robust indicator reflecting the mean climate conditions of the whole Western Amazon basin. We present a more than 200-year long chronology, which is the first ENSO-sensitive dendroclimatic proxy of the Amazon basin and permits the dating of preinstrumental El Niño events. Time series analyses of our data indicate that during the last two centuries the severity of El Niño increased significantly.

Keywords: Amazon, annual tree rings, dendrochronology, El Niño–Southern Oscillation, floodplain forest, paleoclimatology

Received 16 October 2002; revised version received 2 June 2003; and accepted 19 August 2003

Introduction

The El Niño phenomenon, originating from the tropical Pacific Ocean, is the strongest natural interannual climate fluctuation affecting societies and economies of many countries by flooding and severe droughts (Ropelewski & Halpert, 1987; Allan *et al*., 1996). The last two decades have been marked by unusually strong El Niño events in 1982/1983, 1997/1998 and a prolonged activity during 1990–1995. This recent development raised the question whether human-induced 'greenhouse' warming affects the behaviour of the El Niño–Southern Oscillation (ENSO) (Timmermann *et al*., 1999; Houghton *et al*., 2001; Trenberth, 2001). But the historical meteorological Southern Oscillation index (SOI) and oceanographic sea surface temperature (SST) data are of insufficient length to describe the long-term variability of the ENSO (Stahle *et al*., 1998; Mann *et al*., 2000). Therefore, several recent studies focus on the reconstruction of the paleoclimatic ENSO based on long-term instrumental data (Whetton & Rutherfurd, 1994), tree-ring proxies (Jacoby & D'Arrigo, 1990; Stahle *et al*., 1998), isotopic indicators in coral reefs (Dunbar *et al*., 1994; Urban *et al*., 2000; Tudhope *et al*., 2001) and ice cores (Thompson, 1992), or multiproxy combination there of (Mann *et al*., 2000). Despite the ample evidence for annual tree rings in many tropical regions (Worbes, 2002), most dendroclimatic records have been developed in extra-tropical regions, which are too far from the ENSO signal and are influenced by additional atmospheric circulation patterns (Stahle

Correspondance: Dr Martin Worbes, tel. + 00 49 551 39 9504, fax + 00 49 551 39 3759, e-mail: mworbes@gwdg.de

[1]We regret the bereavement of Dr José Márcio Ayres, the founder of the Project Mamirauá for Sustainable Development.

et al., 1998; Enquist & Leffler, 2001). Thus it is not surprising that preinstrumental ENSO reconstructions differ considerably from each other (Quinn & Neal, 1992; Whetton & Rutherfurd, 1994; Stahle *et al.*, 1998). For the tropics where the teleconnection with ENSO is more evident (Trenberth & Caron, 2000) only one long-term dendroclimatical proxy so far exists, constructed by Berlage (1931) with teak on Java. In the over 400-year long chronology, Berlage discovered a cyclic behaviour, which in later reanalysis was confirmed to be ENSO related (Jacoby & D'Arrigo, 1990).

The world's largest remaining tropical forest is the Amazon rain forest. It is severely affected by climatic variations, especially by droughts. Exceptionally low precipitation during the rainy season in the Amazon Basin is generally correlated with the El Niño phenomenon (Adis & Latif, 1996; Tian *et al.*, 1998; Marengo & Nobre, 2001). However, spatial patterns of annual precipitation vary strongly in the Amazon region even on a small scale (Ribeiro & Adis, 1984) and meteorological stations with long-term rainfall records are scarce (Sombroek, 2001). A more robust climate indicator is the daily recorded water level of the Amazon River, representing surface runoff correlated to the mean precipitation in an area of approximately $3\times10^6\,km^2$ of the Andean and Western Amazon watershed (Richey *et al.*, 1989). Seasonal variations in precipitation in the catchment area are displayed by a monomodal flood pulse of the Amazon river with an amplitude up to 14 m (Irion *et al.*, 1997). This leads to an annual extended inundation of floodplains and its forest trees resulting in the formation of annual tree rings (Worbes, 1986, 1997; Schöngart *et al.*, 2002). The existence of annual rings in old trees of the Amazon floodplains opens the possibility to search for climate signals and to reconstruct the climatic conditions of the Amazon Basin for preinstrumental periods.

Material and methods

Tree species and site conditions

From more than 300 tree species in the Amazon floodplains (Worbes, 1997) we chose *Piranhea trifoliata* (Baill.), Euphorbiaceae, as suitable for tree-ring analysis for three reasons:

1. The species is widespread in the whitewater floodplains (*várzea*) of tropical South America. It occurs from the middle Amazon (in Brazil the Rio Solimões) to its mouth into the Atlantic as well as in the Orinoco basin (Worbes *et al.*, 1992).
2. *P. trifoliata* is a frequent hardwood species in mature floodplain forests at low elevations. Individual trees can reach an age of 400 years and more (Worbes & Junk, 1999).
3. The species forms very distinct annual rings (Worbes, 1989), allowing confident tree-ring analysis and age determination.

In total we used 28 stem disc samples for the analysis. Thirteen samples were taken in the year 2000 from sites within the Mamirauá Sustainable Development Reserve close to the City of Tefé, 550 km upstream from Manaus (Fig. 1). The region and the sites are described in more detail in Worbes *et al.* (2001). Fifteen stem discs were taken near Manaus in the year 1986. A detailed description of these sites and the ecological conditions in the Amazon floodplains is available in Worbes *et al.* (1992). The climate of Central Amazonia has a mean temperature of 26.2–26.6 °C and annual precipitation of 2100–2500 mm, characterized by a distinct dry season between June and November (Irion *et al.*, 1997).

Sample preparation, ring-width measurements and data treatment

The stem discs were carefully dried in an air-conditioned room to avoid fungus attack. The surface of the samples was polished with sand paper of decreasing grain size to 600 grit. The wood dust was removed from the vessels with compressed air to improve visibility of the growth zone boundaries. In some cases, it is useful to moisten the surface of the cross-section with some drops of water to increase contrast between different wood tissues and the distinctiveness of growth zones in general.

Ring widths were measured with a digital measuring device to the nearest 0.01 mm. From all samples, up to four radii were measured and the results combined to a 'tree chronology'. In contrast to common dendrochronological usage, all sample numbers refer to these 'tree chronologies' and not to individually measured radii. Standard dendrochronlogical techniques were used to

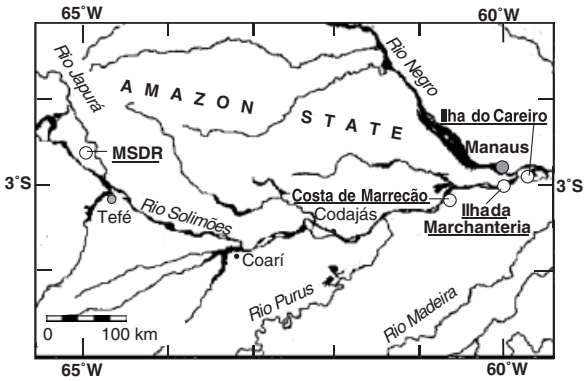

Fig. 1 Overview of the study sites in the Mamirauá Sustainable Development Reserve (MSDR) and along the lower Rio Solimões (Amazon river).

cross-date the tree-ring series of different trees and to combine the individual time series to a master chronology (Stokes & Smiley, 1968). Tree-ring statistics, which describe the similarity of individual curves were performed with the computer program TSAP (Time Series Analysis and Presentation). Measures for the similarity are the Student's *T*-values (Baillie & Pilcher, 1973) and the percentage of parallel run indicating the year-to-year agreement in the oscillation of two curves within the overlapping interval (Schweingruber, 1988). The program also transforms raw ring curves into index curves by removing individual and long-term trends using a 5-year moving average (Fritts, 1976). The residuals of this procedure are normally distributed, which is a basic condition for correlation with climate data (Cook & Briffa, 1990).

Monthly precipitation data were obtained from the climate station in Manaus for the period 1910–1983 since other long-term rainfall records are not available for the study region (Sombroek, 2001). The daily water-level records since 1903 at the port of Manaus together with exact elevations of our study sites were used to calculate the duration of the aquatic phase and the nonflooded period. The relationship between ring widths, local precipitation and flood-pulse data from El Niño events and other years was analysed using two-sample tests. El Niño years were defined by 5-month running means of SST anomalies in the Niño 3.4 region (5°N–5°S/120°–170°W) exceeding 0.4 °C for 6 or more consecutive months (Trenberth, 1997). Records of the SST indices were taken from the data bank of the Climate and Global Dynamics Division (http://www.cgd.ucar.edu/cas/catalog/climind/TNI_N34) (Trenberth & Stepaniak, 2001). The cyclic behaviour of the ups and downs of tree-ring time series was analysed by Fourier analysis. Significance of this analysis was tested with white noise tests (Fuller, 1996) using the programs STATISTICA and SAS. Cross-spectral analysis was performed to determine the relationship between the indexed tree-ring chronology and time series of the SOI (1866–1999) (data: Climatic Research Unit, University of East Anglia) and SST (1871–1999) of the Niño 3.4 Region (Trenberth, 1997) as a function of frequency. A low-pass filter weighted with a Hamming window was used to highlight long-term variations in the tree-ring series (Schweingruber, 1988; Cook & Briffa, 1990).

Results

Tree ring formation and growth periodicity

P. trifoliata is a brevi-deciduous tree species that sheds its leaves during flooding and starts to flush in August at the end of the aquatic phase. Trunk diameter growth occurs mainly in the nonflooded period, with a short depression in November–December, when there is often little precipitation. At the beginning of the aquatic phase diameter increment declines rapidly to zero. These findings indicate the nonflooded period in the floodplain forests as the main vegetation period for *P. trifoliata*. The same holds for many other tree species (Schöngart *et al*., 2002).

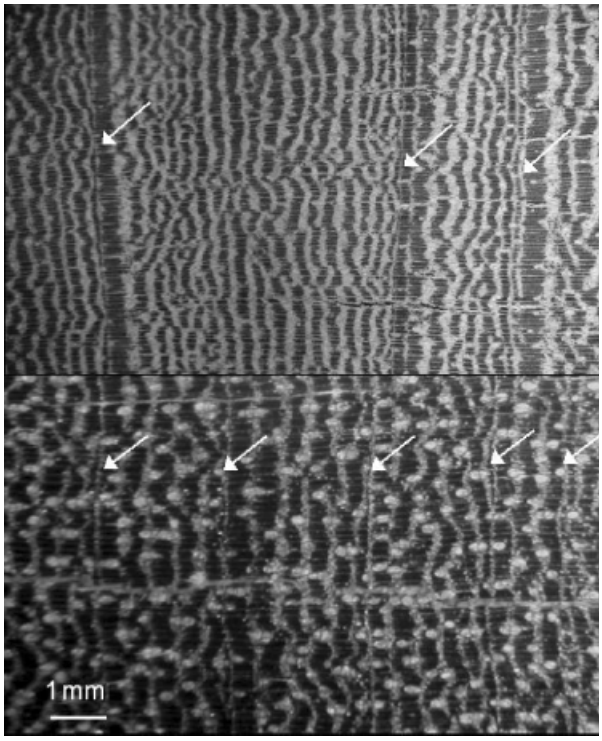

Fig. 2 *Piranhea trifoliata* Baill. (Euphorbiaceae): tree rings characterized by alternating fibre and parenchyma bands (above), in narrow zones annual rings are limited by marginal parenchyma bands (below). Arrows indicate the ring boundaries.

The tree rings of *P. trifoliata* are distinct and of annual nature as shown by radiocarbon dating (Worbes & Junk, 1989). The growth structure is characterized by alternating patterns of fibre and parenchyma tissues (Fig. 2) as often found in Euphorbiaceae. The ring boundaries are formed by terminal parenchyma bands, which run around the entire stem disc. These bands allow the definite identification of the annual rings, even when they are narrow. The width of the rings varies considerably between years from less than 0.4 mm up to more than 6 mm within one individual. The mean ring width across individuals ranges from 1.17 to 4.48 mm (mean of 1.67 mm). The mean age of the investigated trees is 143 years, the oldest tree has an age of 289 years.

Time series analysis and El Niño

The patterns of individual tree-ring curves show good similarities with a mean percentage of parallel run of 64.3% and maximum values up to 76%. The ten best matching tree chronologies (based on 28 radii measurements) were used to construct the master chronology of the Amazon floodplains. The longest individual chronology reaches back to 1697.

For climate analysis the mean chronology was used since the year 1800 where all curves were present. The indexed mean ring-width curve is compared with the precipitation record of Manaus and data derived from the flood pulse (length of aquatic phase, nonflooded period, mean, minimum, maximum flood level and amplitude) (Table 1). There was a weak, but significant negative correlation of $r = -0.36$ ($P < 0.001$) between the ring width and the amount of precipitation during the vegetation period (September–March). The relation between tree growth and the flood pulse, however, is much stronger (Schöngart *et al*., 2002). The chronology correlates negatively with the length of the aquatic phase, the mean and maximum flood level. The strongest climate–growth relation can be detected between the ring width and the duration of the nonflooded period (Fig. 3). The percentage of parallel run between the tree-ring chronology and the length of the nonflooded period is 73%, the correlation with $r = 0.64$ is significant ($P < 0.001$) and high in comparison with results from dendroclimatic analyses in the temperate zones (Schweingruber, 1988).

The teleconnection between the climate variables (precipitation, flood pulse) in the Amazon region and the occurrence of El Niño is shown by two-sample tests (Table 2). Most of the El Niño years peak from November to January in SST of the Niño 3.4 region (Trenberth, 1997) and cause significantly lower precipitation in the rainy season of Central Amazonia with a delay of 2 months (January until March). The teleconnection between climate conditions of the Amazon Basin and El Niño is still more evident in the flood pulse of the Amazon River, which represents the variations of precipitation in the Andean and Western Amazon watershed (Richey *et al*., 1989). A significantly lower water level indicates that El Niño causes negative precipitation anomalies in most parts of the catchment area. Consequently, the vegetation period is extended followed by a shortened aquatic phase. Tree growth responds to the prolonged vegetation period. The ring width in El Niño years is significantly wider compared to neutral years (Table 2).

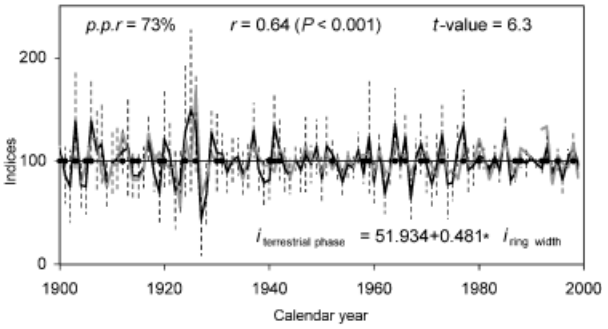

Fig. 3 Indexed ring-width chronology ($n = 10$ stem discs) of *Piranhea trifoliata* (black curve) and deseasonalized time series of the duration of the nonflooded period (grey curve) derived from the daily recorded water level at the port of Manaus. The correlation between the two curves is significant (*p.p.r.* is the percentage of parallel run between the two curves). Vertical lines indicate error bars, black points represent El Niño events. Two-sample tests show significant differences in ring width between ENSO years and neutral years (Table 2).

Table 1 Correlations between indexed ring-width values and climate variables of the flood pulse (1903–1999) and precipitation from Manaus (1910–1983)

Climate variable	*r*	*T*-value
Flood pulse (Rio Solimões)		
Mean water level	−0.32	−3.21*
Maximum water level	−0.29	−2.91*
Minimum water level	−0.05	−0.49
Amplitude	−0.16	−1.56
Aquatic phase	−0.42	−4.31*
Nonflooded period	0.64	6.32*
Precipitation (Manaus)		
Annual rainfall (July–June)	−0.25	−2.14*
Rainfall of vegetation period (September–March)	−0.36	−3.27*

*Significant correlation at the 99.9% confidence level. Data of daily water-level measurements are taken from the Engenharia dos Portos, Manaus, monthly precipitation values from the Instituto Nacional de Meteorologia (INMET).

The indexed ring-width chronology is significantly negatively related to the annual SOI (1866–1999) with $r = -0.29$ ($P < 0.001$). Single spectral analysis and white noise test statistics (Fuller, 1996) describe periodically recurring events in time series. In the 20th century this period is 4.35 years, which matches exactly the average of moderate to very strong El Niño events given by Quinn & Neal (1992) for the period 1925–1982. In the 19th century this period is 3.85 years, but less pronounced than in the following century. This indicates a slight decrease in the periodicity but an increasing strength of the El Niño phenomenon during the last two centuries (Figs 4a, b). Cross-spectral analysis shows that the tree-ring chronology is significantly coherent with instrumental ENSO indices at periods of

Table 2 Two-sample test of climate parameters (precipitation, flood pulse) and ring-width indices between neutral years and those with El Niño events

Parameter	Statistics	ENSO events	Other years	Comparison	Confidence level
Precipitation (mm)	1910–1983	$n = 23$	$n = 50$		
Annual					
July–June	Mean	1882.2	2204.5	*T*-value: −4.10	$P < 0.001$
	SD	±346.3	±295.4	*F*-value: 1.37	NS
January–March	Mean	695.7	888.9	*T*-value: −4.37	$P < 0.001$
	SD	±189.3	±169.1	*F*-value: 1.25	NS
Flood pulse	1903–1999	$n = 32$	$n = 66$		
Flood level (m ASL)	Mean	26.98	28.11	*T*-value: −5.13	$P < 0.001$
	SD	±1.38	±0.80	*F*-value: 0.34	$P < 0.001$
Aquatic phase (days)*	Mean	133	175	*T*-value: −5.07	$P < 0.001$
	SD	±46	±34	*F*-value: 0.55	$P < 0.05$
Nonflooded period (days)*	Mean	223	197	*T*-value: 3.35	$P < 0.001$
	SD	±39	±33	*F*-value: 0.71	NS
Ring-width indices	1872–1999	$n = 43$	$n = 85$		
Instrumental period	Mean	104.2	97.2	*T*-value: 4.26	$P < 0.001$
	SD	±8.3	±8.9	*F*-value: 1.16	NS

The differences between mean and standard deviations (SDs) were examined for the instrumental record by *T*-tests and *F*-tests, respectively (NS, not significant).
*Calculated for the mean elevation of the study sites at 24.38 m ASL.

11.6, 6.7–7.1, 5.6–5.8, 3.0–3.2 and 2.2–2.1 years from SST of the Niño 3.4 region (Fig. 4c). The chronology shows almost identical frequency bands with the SOI (12.6–14.0, 7.0–7.4, 5.5–5.7, 3.3–3.6, 3.1–3.2 and 2.1 years, not shown). At these periodicities, more than 60% of the ring-width variance correlates linearly to the ENSO. To explore the decadal-to-interdecadal variability of the ENSO, the tree-ring chronology is smoothed with a low-pass filter (moving average) weighted with a Hamming window (Fig. 5). The low-pass filter indicates a high El Niño activity in the first two decades of the 19th century and a less active period during the middle of the 19th century for more than 50 years (Fig. 4).

Discussion

Diameter increment of trees in the Amazon floodplains is triggered by the annual flood pulse and mainly restricted to the nonflooded period (Worbes, 1997; Schöngart *et al*., 2002). This explains the close relation between the duration of the vegetation period and the ring width of *P. trifoliata* as well as other tree species of the floodplain forests (Worbes, 1988, Worbes *et al*., 1995, Dezzeo *et al*., 2003). In this study we can associate this climate-growth relation successfully to the El Niño phenomenon that causes severe drought in large parts of the Amazon basin (Nepstad *et al*., 1999; Marengo & Nobre, 2001; Sombroek, 2001).

In nonflooded 'terra firme' forests diameter increment of trees is positively correlated with the amount of local precipitation (Jacoby & D'Arrigo, 1990; Stahle *et al*., 1999; Worbes, 1999). The drier and warmer climate conditions during an El Niño cause a decreased soil moisture in 'terra firme' forests leading to reduced photosynthesis, increased respiration rates and to a lower net primary production (Tian *et al*., 1998). Therefore, most parts of the 'terra firme' forests act as a carbon source during an El Niño event (Prentice & Lloyd, 1998). Floodplain forests, however, show increased wood growth and thus may absorb some of the El Niño-induced carbon releases of Amazon 'terra firme' forests. This duality has not been considered in existing estimates of carbon fluxes based on biogeochemical models, measurements of gas fluxes or accumulation of carbon in vegetation and soils.

The presented tree-ring chronology is the first ENSO-sensitive proxy from the Amazon basin and the second longest dendroclimatic proxy of the tropics developed so far. Seventy percent of the instrumental El Niño events can be detected in our dendroclimatic record. This is a high value in comparison with recent multivariate proxies, which explain less than 50% of all instrumentally recorded El Niño years (Stahle *et al*., 1998). The strong El Niño phenomenon in 1925/1926 (Quinn & Neal, 1992), for instance, is represented by the lowest flood level on record that appears as a distinct peak in the dendroclimatic proxy (Fig. 3). Exceptional droughts and large-scale fires are reported during 1925–1927 in the 'terra firme' forests of the catchment area and along the lower course of the Rio Negro

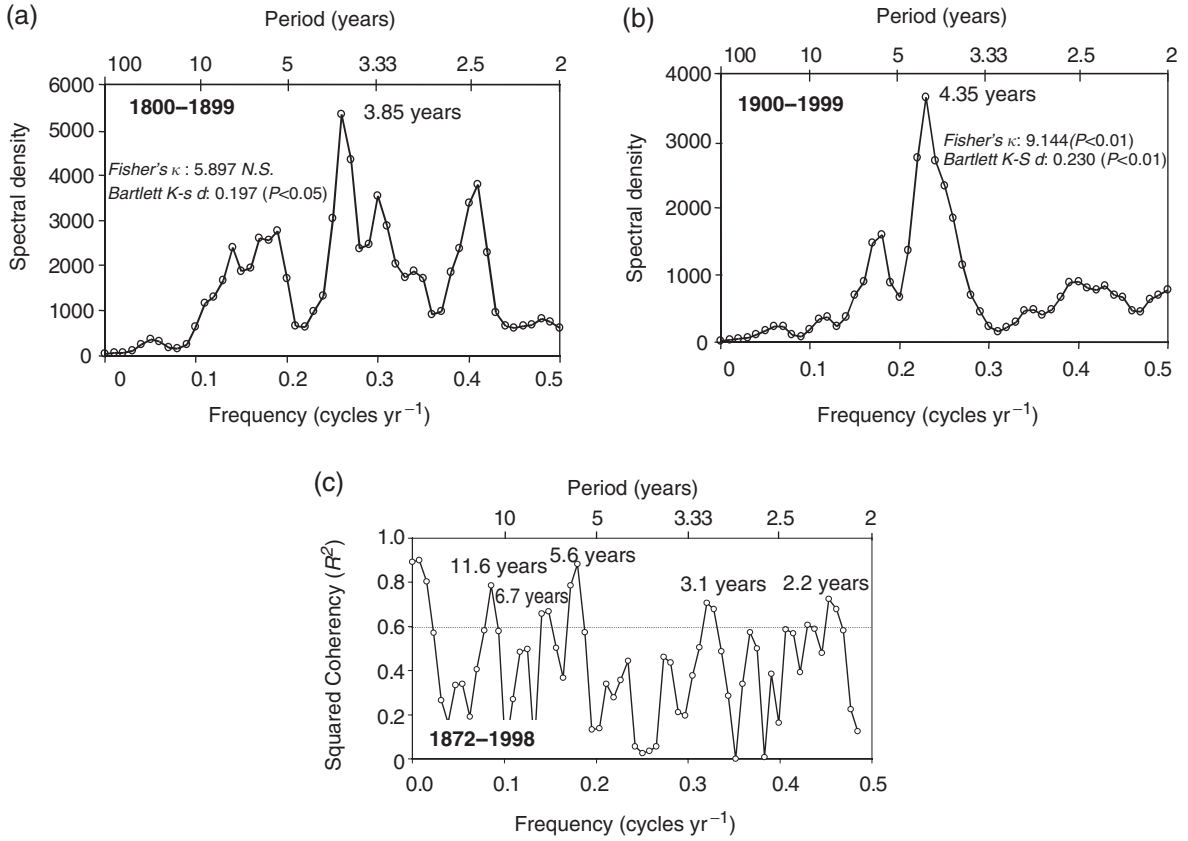

Fig. 4 Single spectrum analysis of the indexed ring-width chronology computed for (a) the 19th century and (b),the last century. The ring-width time series was smoothed using a Hamming window with a bandwidth of 2 years. White noise tests (Fisher's κ test and Bartlett Kolmogorov–Smirnov statistics) indicate if the time series includes a significant cycle (NS, not significant). (c) Cross-spectral analysis between the indexed ring-width chronology and the Sea Surface Temperature during November–January of the Niño 3.4 region (Trenberth, 1997) for the instrumental period 1872–1999.

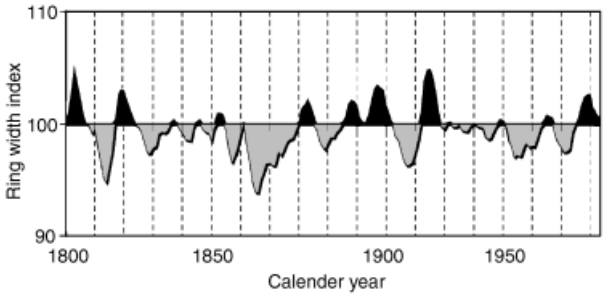

Fig. 5 Ring-width chronology of *Piranhea trifoliata* smoothed with a low-pass filter weighted with a Hamming window (bandwidth of 12 years) to explore warm ENSO (black) and cool ENSO phases (grey).

(Sternberg, 1987; Sombroek, 2001). The severe El Niños of 1982/1983 and 1997/1998 appear only as small peaks in the dendroclimatic record. Both events caused significantly less rainfall in Central Amazonia (Sombroek, 2001). The flood pulse, however, does not show distinct anomalies during these events. In 1998 the maximum water level of the Amazon River at Manaus was 27.58 m ASL, even higher than the mean value of 26.98 m ASL for other El Niño years (Table 2). Consequently, the nonflooded period in 1997/1998 was short and the signal in the chronology is weaker compared to other El Niño events. Further dendroclimatic studies should therefore include sites along tributaries of the Amazon River with catchment areas in Central and Northern Amazonia where the El Niño signal is more pronounced (Marengo & Nobre, 2001).

The nonflooded period starts within the dry season. In years with a delayed onset of rains, tree growth of *P. trifoliata* and other tree species often decreases at the end of the dry season in November/December (Schöngart *et al.*, 2002), when the soil water content in floodplain forests declines sometimes close to the permanent wilting point (Worbes, 1986). In those years, tree growth thus may not perfectly coincide with the length of the vegetation period.

We find parallels between our results and those from studies based on other independent proxy data

Table 3 Comparison of cycles derived from spectral analysis between El Niño indicators (SOI, SST) and different instrumental records and proxies mainly developed in tropical regions

Reference	Location	Variables	Method	Period	Cycles yr^{-1}
Meteorological and hydrological data					
Adis & Latif (1996)	Central Amazonia	Precipitation (Manaus) and SOI	Cross-spectral	1910–1983	2.4
Richey *et al*. (1989)		Surface runoff (Amazonas) and SOI	Cross-spectral	1903–1985	2–3
Historical records					
Quinn & Neal (1992)	West coast of South America	Moderate–very strong El Niño events	Average	1803–1982 1525–1982 1925–1982	3.8 5.5 4.4
		Strong–very strong El Niño events	Average	1925–1982	11.4
Dendroclimatic proxies					
This study	Central Amazonia	Ring-width index and SST (Niño 3.4)	Cross-spectral	1872–1998	2.1–2.2, 2.3, 3.0–3.2, 5.6–5.8, 6.7–7.1, 11.6
		Ring-width index	Single spectral	1900–1999 1800–1899	4.35 3.85
Stahle *et al*. (1998)	JavaSouthwest of North America	Instrumental and reconstructed SOI	Cross-spectral	1877–1977	2.3, 3.8
		Instrumental SOI	Single spectral	1706–1977	3.85, 6.25
		Reconstructed SOI	Single spectral	1706–1977	4.0, 5.7
Coral-based isotopes					
Cole *et al*. (1993)	Tropical Pacific	δO^{18} isotopes with SOI and SST	Cross-spectral	1893–1989	1.9–2.3, 3.0, 3.6, 5.6
Urban *et al*. (2000)		δO^{18} isotopes and SST (Niño 3.4)	Cross-spectral	1856–1995	2.2–2.4, 2.5–2.8, 3.3–3.8, 4.7–6, 10–15

The average of El Niño events for different time periods is calculated for the chronology of Quinn & Neal (1992) based on historical documentation.
SOI, Southern Oscillation index; SST, sea surface temperature.

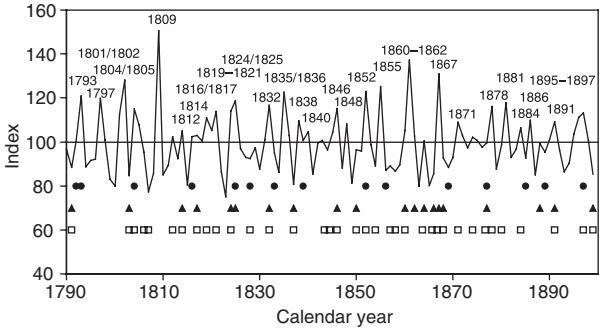

Fig. 6 Reconstruction of the duration of the nonflooded period to the year 1790 using a linear regression model for calibration (Fig. 3). Calendar years indicate reconstructed El Niño events (index values $\geq$104.2) (Table 1). The time series is compared with El Niño events derived from dendroclimatic records (circles, Stahle *et al*., 1998), long-term instrumental data from Africa, India and Northern China (triangles, Whetton & Rutherfurd, 1994), and historical accounts in the coastal equatorial zone of Peru and Ecuador (squares, Quinn & Neal, 1992).

evaluated in the tropics. The significant correlation between the annual SOI and the ring width is not very high but comparable to correlations between the SOI and other proxies based on tree rings (Lough & Fritts, 1985; Jacoby & D'Arrigo, 1990), long-term instrumental records (Whetton & Rutherfurd, 1994) and isotopic indicators derived from corals (Dunbar *et al*., 1994) and ice cores (Thompson, 1992). The correlation between the SST and the tree-ring chronology in the frequency band of 2–12 cycles yr^{-1} are also visible in the ENSO-sensitive time series of coral-based δO^{18} isotopes close to the Niño 3.4 region (Cole *et al*., 1993; Urban *et al*., 2000) (Table 3). This confirms the association between the dendroclimatic record from the Amazonian floodplains and the variations in the SST of the Niño 3.4 region. Our tree-ring chronology is a robust indicator reflecting the basinwide precipitation conditions and their teleconnection with the ENSO.

The close relation between tree growth and climate allows the reconstruction of the duration of the

nonflooded period in the 19th century with a linear regression model (Fig. 6). From this reconstruction we derived El Niño years and compared them with a reconstruction of El Niño events based on a multilingual historical documentation along the Pacific coast of Ecuador and Peru (Quinn & Neal, 1992), a multiproxy from the Eastern hemisphere developed from tree rings from Java, long-term instrumental data of Africa, India and North China (Whetton & Rutherfurd, 1994), and dendroclimatic proxies mainly from the Southwest of North America (Stahle *et al*., 1998). For the period 1790–1900 we found a congruence of 52% and 47% with the dated El Niño years of Whetton & Rutherfurd (1994) and Quinn & Neal (1992), respectively, higher than with tree-ring-based proxies from the subtropical regions, where additional atmospheric circulation (e.g. North Atlantic Oscillation) can overlay the El Niño-induced climate anomalies (Enquist & Leffler, 2001). Therefore, these proxies may not coincide with the variability of the ENSO. In certain periods, however, the coincidence is much higher, e.g. from 1793 to 1832, when nearly all dated El Niño years from Quinn & Neal (1992), Whetton & Rutherfurd (1994) and Stahle *et al*. (1998) appear in our reconstruction. The high congruence among the proxies during this period indicates a warm ENSO phase as also highlighted in the low-pass filter (Fig. 5). The same is true for the last decades of the 19th century, when our postulated El Niño years reappear in the proxies from other authors (Fig. 6). The weak ENSO activity shown by the low-pass filter from 1825 to 1865 is also seen in Sr/Ca variability in corals from the Southern Pacific Ocean (Linsley *et al*., 2000) and mid-latitude tree-ring chronologies from North and South America (Evans *et al*., 2000). Such changes in the lower frequency of the ENSO may be modulated by the Pacific Decadal Oscillation (PDO) of the Northern Pacific, which is connected to the tropical and southern hemisphere climate (Mantua *et al*., 1997).

In total our findings accurately show varying activities of El Niño in the last two centuries. The general trend is an increase of El Niño events from the 19th to the 20th century in the Amazon basin. Severe droughts provoked by El Niño increase the fire risk of large areas of 'terra firme' forests experiencing high rates of logging and fragmentation (Laurance *et al*., 2001). Large-scale fires release huge amounts of greenhouse gases (Nepstad *et al*., 1999; Cochrane, 2003), which feed back and accelerate climate changes (Houghton *et al*., 2001) and probably increase the strength of the ENSO (Timmermann *et al*., 1999).

The demonstrated ENSO-sensitive record from the Amazon River floodplains indicates the great potential of dendroclimatological investigations to obtain more reliable, accurately dated time series. There is evidence of an annual growth rhythm triggered by precipitation patterns in most tropical regions and many tree species are suitable for further dendrochronological studies (Détienne, 1989; Worbes, 2002). Hence, future research should focus more on these regions where teleconnections to the ENSO are more evident to create a dendroclimatic network of climate-sensitive records for the tropical belt for a better understanding of climate changes in the tropics. Together with δO_{18} coral-based indicators, historical archives and long-term instrumental data, a comprehensive network of dendroclimatic records from tropical regions could utilize the approach of multiproxies to reconstruct the ENSO beyond the period of instrumental oceanographic and meteorological records as it was done for the North Atlantic Oscillation (Cullen *et al*., 2001).

Acknowledgements

This work is part of the SHIFT-Program and the LBA and was conducted in co-operation between the Amazon Research Institute (INPA), Manaus, Brazil, and the Working Group Tropical Ecology of the Max-Planck Institute for Limnology, Plön, Germany. We greatly acknowledge the financial support of the Brazilian Research Council (CNPq) and the German Ministry of Science and Technology (BMBF). We are indebted to Prof. Dr Holm Tiessen, Göttingen, for his linguistic help. We also thank two referees for valuable comments to improve the manuscript.

References

Adis J, Latif M (1996) Amazonian arthropods respond to El Niño. *Biotropica*, **28**, 403–408.

Allan RJ, Lindesay J, Parker DE (1996) *El Niño-Southern Oscillation and Climatic Variability*. CSIRO Publishing, Melbourne.

Baillie MGL, Pilcher JR (1973) A simple crossdating programme for tree-ring research. *Tree-Ring Bulletin*, **33**, 7–14.

Berlage HP (1931) Over het verband tusschen de dikte der jaarringen van djatiboomen (*Tectona grandis* L.F.) en den regenval op Java. *Tectona*, **24**, 939–953.

Cochrane MA (2003) Fire science for rainforests. *Nature*, **421**, 913–919.

Cole JE, Fairbanks RG, Shen GT (1993) Recent variability in the Southern Oscillation: isotopic results from a Tarawa atoll coral. *Science*, **260**, 1790–1793.

Cook ER, Briffa K (1990) Data analysis. In: *Methods of Dendrochronology, Applications in the Environmental Sciences* (eds Cook ER, Kairiukstis LA), pp. 97–162. Kluwer Academic Publishers, Dordrecht, Boston, London.

Cullen H, D'Arrigo R, Cook E *et al*. (2001) Multiproxy-based reconstructions of the North Atlantic Oscillation over the past three centuries. *Paleoceanography*, **15**, 27–39.

Détienne P (1989) Appearance and periodicity of growth rings in some tropical woods. *IAWA Bulletin*, **10**, 123–132.

Dezzeo N, Worbes M, Ishii I *et al*. (2003) Growth rings analysis of four tropical tree species in seasonally flooded forest of Mapire River, a tributary of the lower Orinoco River, Venezuela. *Plant Ecology*, **168**, 165–175.

Dunbar RB, Wellington GM, Colgan MW *et al*. (1994) Eastern Pacific surface temperature since 1600 A.D. The $\delta^{18}O$ record of climate variability in the Galapagos corals. *Paleoceanography*, **9**, 291–315.

Enquist BJ, Leffler AJ (2001) Long-term tree ring chronologies from sympatric tropical dry-forest trees: individualistic responses to climatic variation. *Forest Ecology and Management*, **17**, 41–60.

Evans MN, Kaplan A, Cane DP *et al*. (2000) Globality and optimality in climate field reconstructions from proxy data. In: *Present and Past Inter-Hemispheric Climate Linkages in the Americas and their Social Effects* (ed. Markgraf V), pp. 53–72. Cambridge University Press, Cambridge, UK.

Fritts HC (1976) *Tree Rings and Climate*. Academic Press, London.

Fuller WA (1996) *Introduction to Statistical Time Series*, 2nd edn. John Wiley, New York.

Houghton JT, Ding Y, Griggs DJ *et al*. (2001) *Climate Change 2001: The Scientific Basis. Contribution of Working Group I to the Third Assessment Report of the Intergovernmental Panel on Climate Change (IPCC)*. Cambridge University Press, UK.

Irion G, Junk WJ, Mello JASN de (1997) The large Central Amazonian river floodplains near Manaus: geological, climatological, hydrological, and geomorphological aspects. In: *The Central Amazon Floodplains. Ecology of a Pulsing System* (ed. Junk W), pp. 23–46. Springer Verlag, Berlin, Heidelberg, New York.

Jacoby GC, D'Arrigo RD (1990) Teak (*Tectona grandis* L.F.), a tropical species of large-scale dendroclimatic potential. *Dendrochronologia*, **8**, 83–98.

Laurance WF, Williamson GB, Delamônica P *et al*. (2001) Effects of a strong drought on Amazonian forest fragments and edges. *Journal of Tropical Ecology*, **17**, 771–785.

Linsley BK, Wellington GM, Schrag DP (2000) Decadal sea surface temperature variability in the subtropical South Pacific from 1726 to 1997 A.D. *Science*, **290**, 1145–1148.

Lough JM, Fritts HC (1985) The Southern Oscillation and tree rings: 1600–1961. *Journal of Climate and Applied Meteorology*, **24**, 952–966.

Mann ME, Bradley RS, Hughes MK (2000) Long-term variability in the El Niño/Southern Oscillation and associated teleconnections. In: *El Niño and the Southern Oscillation: Multiscale Variability and its Impacts on Natural Ecosystems and Society* (eds Diaz HF, Markgraf V), pp. 357–412. Cambridge University Press, Cambridge.

Mantua NJ, Hare SR, Zhang Y *et al*. (1997) A Pacific interdecadal climate oscillation with impacts on salmon production. *Bulletin of the American Meteorological Society*, **78**, 1069–1079.

Marengo JA, Nobre CA (2001) General characteristics and variability of climate in the Amazon Basin and its links to the global climate system. In: *The Biogeochemistry of the Amazon Basin* (eds McClain ME, Victoria RL, Richey JE), pp. 17–41. Oxford University Press, Oxford.

Nepstad D, Veríssimo A, Alencar A *et al*. (1999) Large-scale impoverishment of Amazonian forests by logging and fire. *Nature*, **398**, 505–508.

Prentice IC, Lloyd J (1998) C-quest in the Amazon Basin. *Nature*, **396**, 619–620.

Quinn WH, Neal VT (1992) The historical record of El Niño events. In: *Climate since A.D. 1500* (eds Bradley RS, Jones PD), pp. 623–648. Routledge, London.

Ribeiro M, de NG, Adis J (1984) Local rainfall variability – a potential bias for bioecological studies in the Central Amazon. *Acta Amazonica*, **14**, 159–174.

Richey JE, Nobre C, Deser C (1989) Amazon river discharge and climate variability: 1903–1985. *Science*, **246**, 101–103.

Ropelewski CF, Halpert MS (1987) Global and regional scale precipitation patterns associated with the El Niño/Southern Oscillation. *Monthly Weather Review*, **115**, 1606–1626.

Schöngart J, Piedade MTF, Ludwigshausen S *et al*. (2002) Phenology and stem-growth periodicity of tree species in Amazonian floodplain forests. *Journal of Tropical Ecology*, **18**, 581–597.

Schweingruber FH (1988) *Tree Rings*. Reidel, Dordrecht, the Netherlands.

Sombroek W (2001) Spatial and temporal patterns of Amazon rainfall. *Ambio*, **30**, 388–396.

Stahle DW, D'Arrigo RD, Krusic MK *et al*. (1998) Experimental dendroclimatic reconstruction of the Southern Oscillation. *Bulletin of the American Meteorological Society*, **79**, 2137–2152.

Stahle DW, Mushove PT, Cleaveland MK *et al*. (1999) Management implications of annual growth rings in *Pterocarpus angolensis* from Zimbabwe. *Forest Ecology and Management*, **124**, 217–229.

Sternberg H O'R (1987) Aggravation of floods in the Amazon River as a consequence of deforestation? *Geografiska Annaler*, **69A**, 201–219.

Stokes MA, Smiley TL (1968) *An Introduction to Tree-Ring Dating*. University of Chicago Press, Chicago.

Thompson LG (1992) Ice core evidence from Peru and China. In: *Climate since A.D. 1500* (eds Bradley RS, Jones PD), pp. 517–548. Routledge, London.

Tian H, Melillo JM, Kicklighter DW *et al*. (1998) Effect of interannual climate variability on carbon storage in Amazonian ecosystems. *Nature*, **396**, 664–667.

Timmermann A, Oberhuber J, Bacher A *et al*. (1999) Increased El Niño frequency in a climate model forced by future greenhouse warming. *Nature*, **398**, 694–697.

Trenberth KE (1997) The definition of El Niño. *Bulletin of the American Meteorological Society*, **78**, 2771–2777.

Trenberth KE (2001) Stronger evidence of human influences on climate: the 2001 IPCC Assessment. *Environment*, **43**, 8–19.

Trenberth KE, Caron JM (2000) The Southern Oscillation revisited: sea level pressures, surface temperature, and precipitation. *Journal of Climate*, **13**, 4358–4365.

Trenberth KE, Stepaniak DP (2001) Indices of El Niño evolution. *Journal of Climate*, **14**, 1697–1701.

Tudhope AW, Chilcott CP, McCulloch MT *et al*. (2001) Variability in the El Niño-Southern Oscillation through a glacial–interglacial cycle. *Science*, **291**, 1511–1517.

Urban FE, Cole JE, Overpeck JT (2000) Influence of mean climate change on climatic variability from a 155 yr tropical Pacific coral record. *Nature*, **407**, 989–993.

Whetton P, Rutherfurd I (1994) Historical ENSO teleconnection in the eastern hemisphere. *Climatic Change*, **28**, 221–253.

Worbes M (1986) Lebensbedingungen und Holzwachstum in zentralamazonischen Überschwemmungswäldern. *Scripta Geobotanica*, **17**, 1–112.

Worbes M (1988) Variety in structure of annual growth zones in *Tabebuia barbata* (E. Mey.) Sandw., Bignoniaceae, a tropical tree species from Central Amazonian inundation forests. *Dendrochronologia*, **6**, 71–89.

Worbes M (1989) Growth rings, increment and age of trees in inundation forests, savannas and a mountain forest in the Neotropics. *IAWA Bulletin n.s.*, **10**, 109–122.

Worbes M (1997) The forest ecosystem of the floodplains. In: *The Central Amazon Floodplains. Ecology of a Pulsing System* (ed. Junk WJ), pp. 223–266. Springer Verlag, Berlin, Heidelberg, New York.

Worbes M (1999) Annual growth rings, rainfall-dependent growth and long-term growth patterns of tropical trees from the Caparo Forest Reserve in Venezuela. *Journal of Ecology*, **87**, 391–403.

Worbes M (2002) One hundred years of tree-ring research in the tropics – a brief history and an outlook to future challenges. *Dendrochronologia*, **20**, 217–231.

Worbes M, Junk WJ (1989) Dating tropical trees by means of ^{14}C from bomb tests. *Ecology*, **70**, 503–507.

Worbes M, Junk WJ (1999) How old are tropical trees? The persistence of a myth. *IAWA Journal*, **20**, 255–260.

Worbes M, Klinge H, Revilla JD *et al*. 1992 On the dynamics, floristic subdivision and geographical distribution of várzea forests in Central Amazonia. *Journal of Vegetation Science*, **3**, 553–564.

Worbes M, Klosa D, Lewark S (1995) Rohdichtestruktur von Jahresringen tropischer Hölzer aus zentralamazonischen Überschwemmungswäldern. *Holz als Roh- und Werkstoff*, **53**, 63–67.

Worbes M, Piedade MTF, Schöngart J (2001) Holzwirtschaft im Mamirauá-Projekt zur nachhaltigen Entwicklung einer Region im Überschwemmungsbereich des Amazonas. *Forstarchiv*, **72**, 188–200.